RSC Advances

PAPER

Check for updates

Ion-triggered calcium hydroxide microcapsules for enhanced corrosion resistance of steel bars†

Zi Liang,[ab] Qian Wang, ID *[b] Biqin Dong,[a] Bingyin Jiang[b] and Feng Xing*[a]

Herein, we synthesized $Ca(OH)_2$ microcapsules with ion-responsive shells composed of cross-linked poly-ionic liquids (CPILs). By exchanging PF_6^- with Cl^- in water, the hydrophobic poly-ionic liquids (PILs) on the shell are converted to hydrophilic channels. The encapsulated $Ca(OH)_2$ can permeate through the hydrophilic channels and release OH^-. Meanwhile, the Cl^- content can be reduced. The release rate of $Ca(OH)_2$ is influenced by the content of monomers and concentration of Cl^- ions in water. SO_4^{2-} can also trigger the release of $Ca(OH)_2$ from the microcapsule. With these microcapsules, Q235 steel exhibited promising corrosion resistance in simulated seawater. These results indicate that encapsulation of corrosion inhibitors is highly desirable for enhanced corrosion resistance of steel bars and the proposed approach can be used to encapsulate various corrosion inhibitors and functional materials for a wide range of applications.

Introduction

Corrosion of reinforced concrete can greatly threaten the durability of reinforced concrete structures.[1–5] In seawater, chloride (Cl^-) ions are a major cause of the corrosion of steel reinforcement embedded in concrete.[6,7] The Cl^- ions can penetrate through the bulk concrete matrix and reach the steel/concrete interface. When the Cl^- ions concentration exceeds a threshold, the surface protective passive layer of steel is destroyed and comes under attack by the Cl^- ions.[4,8–11] It has been reported that the corrosion rate increases when the Cl^-/OH^- ratio is higher than a critical value,[12–14] that is, the protection of steel will be significant by simultaneously lowering the Cl^- concentration and increasing the OH^- concentration, which provides a key design parameter for corrosion reduction. Many commercially available corrosion inhibitors are used to inhibit chlorides induced corrosion, such as chromates and heavy metals. Unfortunately, they are usually toxic and hazardous. Therefore, eco-friendly corrosion inhibitors, such as calcium hydroxide ($Ca(OH)_2$) and sodium monofluorophosphate (Na_2PO_3F), are considered promising and have gained significant research focus.[15,16] The inexpensive $Ca(OH)_2$ can effectively inhibit the corrosion by increasing the local pH value of concrete solution.[17] However, the corrosion inhibitor may be dissolved before the Cl^- ions affect the steel. Moreover,

the large amount of calcium hydroxide can also inhibit the hydration process of cement, which further reduces the performance of concrete. Therefore, the effective encapsulation of corrosion inhibitor is required to control the release. There have been many reports on encapsulation of the corrosion inhibitors, where the release is triggered by pH[18–20] or crack.[21,22] Matsuda *et al.* has synthesized pH-sensitive microcapsules with a shell composed of ester chains with the ability to be hydrolyzed in both alkaline and acidic, which can form oxide layer on the steel substrate. Wang *et al.* fabricated a self-immunity ethyl cellulose (EC)/calcium hydroxide microcapsule which can be triggered by low pH values, and calcium hydroxide can be controllably released to regulate the environmental pH condition. The EC shell of the microcapsule is not pH-responsive. The key to trigger the release is the low concentration of hydroxide in the solution. Yang *et al.* has synthesized methylmethacrylate or triethylborane core/silica gel shell microcapsules. The crack in concrete ruptures the microcapsules and the healing agent contacts the catalyst, triggering polymerization that bonds the crack. However, it is difficult to adjust local pH or initiate cracking under marine environment. Thus, the release of corrosion inhibitors triggered by Cl^- ions is highly desirable because it is the most abundant anion in the seawater.[23,24] Based on these, it is highly desirable to synthesize a capsule of $Ca(OH)_2$ with a Cl^- responsive shell to protect the steel under marine environment.

Recently, the ionic liquids (ILs) have attracted considerable research attention due to their advantageous properties, for example, high ionic conductivity, chemical stability and flame resistance.[25–27] The anions of ILs can be exchanged with other anions, such as the typical Cl^-, which enables the ILs experience hydrophobic–hydrophilic conversion.[25,28] With the

*School of Civil Engineering, Guangdong Province Key Laboratory of Durability for Marine Civil Engineering, Shenzhen University, Shenzhen 518060, China. E-mail: xingf@szu.edu.cn

*State Key Laboratory of Polymer Physics and Chemistry, Institute of Chemistry, Chinese Academy of Sciences, Beijing 100190, China. E-mail: wangqian@iccas.ac.cn

† Electronic supplementary information (ESI) available. See DOI: 10.1039/c8ra07382a

responsiveness to Cl^-, ILs is considered suitable to be used as the Cl^- responsive shell.

Herein, we have synthesized $Ca(OH)_2$ microcapsules with an ion-responsive cross-linked poly-ionic liquids (CPILs) shell. By exchanging the anions of the PILs with aggressive anions such as Cl^- or sulfate (SO_4^{2-}), the hydrophobic PILs on the shell convert to hydrophilic. The $Ca(OH)_2$ has relatively low water solubility and it can gradually permeate outside the microcapsule through the shell. During the permeation process, the $Ca(OH)_2$ passes through the hydrophilic channels, where anions of the PILs are exchanged by Cl^- (Fig. 1). We have observed the morphology of microcapsules by scanning/transmission electron microscopy (SEM/TEM) and analyzed the structure of microcapsules by X-ray diffraction (XRD) and energy dispersive X-ray (EDX) before and after Cl^--trigger to verify the ion-responsive of microcapsules. The UV-vis was used to measure the concentration of Ca^{2+} after anion-trigger in order to study the influence of the monomers content and Cl^- concentration on the release rate of $Ca(OH)_2$. Finally, the corrosion resistance of steel bars was studied under simulated marine environment.

Experimental

Materials

The dimethylformamide (DMF) and ethanol were purchased from Beijing Chemical Works. The maleic anhydride (MA), $Ca(OH)_2$, sodium chloride (NaCl) and potassium bromide (KBr) were purchased from Sinopharm Chemical Reagent. The azobisisobutyronitrile (AIBN) was purchased from J&K Chemical. The ionic liquid 1-vinyl-3-ethylimidazolium hexafluorophosphate ($VEImPF_6^-$) was supplied by Lanzhou Institute of Chemical Physics. The phenolphthalein was purchased from Beijing Modern Fine Chemicals. The methylthymol blue (MTB)

was purchased from Nanjing Jiancheng Bioengineering Institute. The above reagents were used as received. The divinylbenzene (DVB) and styrene (St) were purchased from Sigma-Aldrich and purified by Al_2O_3 to remove inhibitor before use.

Synthesis of the microcapsules

The $Ca(OH)_2$ was grounded and sieved to remove larger particles. 1 g of $Ca(OH)_2$ powder was dispersed in 40 mL DMF solution containing 0.045 g of MA and purged with N_2 for 30 min. Then 0.3 g of St, 0.454 g of DVB and 0.01 g of AIBN were added into the dispersion under stirring. Subsequently, 0.2 g of $VEImPF_6^-$, dissolved in DMF, was added to the above suspension. The reaction was continued at 70 °C with N_2 for 24 h under continuous stirring. The product was washed with DMF for three times and the brown microcapsule powder was obtained after desiccation. The microcapsules with different contents of monomers were synthesized (Table S1†).

Ion responsiveness

12 mg of microcapsules were added to 30 mL of NaCl solution with different concentrations. The NaCl solution was purged with N_2 for 30 min to exclude CO_2 before use. 50 μL of the suspension was periodically taken out and dropped into an alkaline solution of MTB (1 mL MTB and 2 mL alkaline solution) for ultraviolet-visible spectroscopy test. MTB was used as a coloring agent and the absorbance of the resultant colored Ca–MTB complex was monitored at 610 nm.[29] The SO_4^{2-} responsiveness of microcapsule was also tested with the same method.

Corrosion resistance of steel

To investigate the corrosion resistance of the microcapsules, the Q235 steel bar with length of 10 cm and diameter of 0.98 cm was selected as a working electrode to perform accelerated corrosion
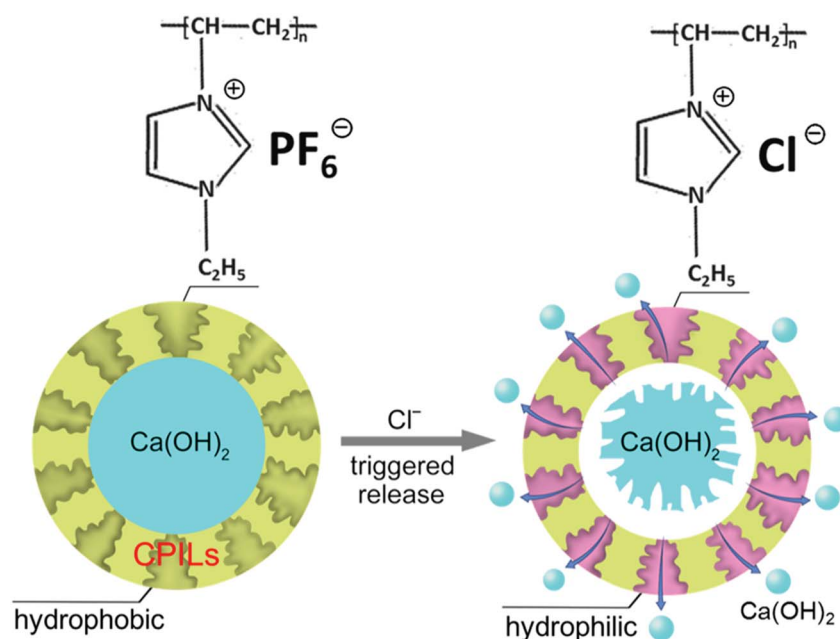

Fig. 1 Schematic illustration of the release process of $Ca(OH)_2$ from the microcapsules triggered by Cl^-.

tests. The composition of the steel was confirmed by X-ray fluorescence spectroscopy (XRF) (Table S2†). The samples were prepared as follows: (1) the surface of steel bar was sealed by water repellent tape and epoxy; (2) one end of the steel bar was punched and welded by wire; (3) the other end of the steel bar was exposed to simulated seawater for corrosion. The 3.5 wt% NaCl in deionized water was used to imitate the marine environment. Different contents of microcapsules were added to the solution to investigate the anti-corrosion capacity. The exposed working area was compared after 60 d.

In most of the corrosion related studies, the mass loss measurement is an accurate and precise method to evaluate corrosion. The mass loss can be obtained by using the gravimetric method, which compares the mass of the steel before and after corrosion.[30] According to the Chinese Standard GB/T 50082-2009, the steel mass is measured as follows: first, the steel was pickled in 12 wt% HCl solution and washed with water. After neutralization in limewater, the steel was washed with water again. Then, the cleaned steel is dried in an oven for 4 h and then weighed (the quality is accurate to 0.001 g).

Characterization

The Fourier transform infrared (FTIR) spectroscopy was carried out by using KBr containing pressed pellets. The samples were scanned for 32 times by using a Bruker EQUINOX 55 spectrometer. The XRD patterns were recorded on a Rigaku D/max 2500 powder X-ray diffractometer. The XRD scan was carried out in the range of 10–80° at a scan speed of 5° min^{-1}. The morphology of the microcapsules and residue samples was characterized by

SEM (Hitachi S-4800 at 15 kV), equipped with an EDX analyzer, and TEM (JEOL 1011 at 100 kV). The samples were vacuum sputtered with Pt prior to SEM observations. The TEM samples were prepared by spreading dilute dispersion in ethanol onto carbon-coated copper grids. The pH of microcapsule aqueous suspension was measured by pen-tape pH detector (SX-pH170, Beijing Heng Odd Instrument Company). The calcium (Ca^{2+}) ions concentration in deionized water was obtained by the colorimetric method by using Ultraviolet-visible spectroscopy (UV-vis, Lambda 950). The deionized water was used as a reference. The Cl^- concentration was measured by chloride-ion meter (XSCL, Beijing Heng Odd Instrument Company).

Results and discussion

Preparation and characterization of microcapsules

$Ca(OH)_2$ particles are rough with irregular contours. The size distribution is broad, ranging from nanometers to micrometers (Fig. 2a and b). MA is preferentially absorbed onto the calcium hydroxide particle surface via hydrogen bonding between MA and hydroxyl group of calcium hydroxide. Since MA is not self-polymerizable, and MA can be copolymerized with DVB,[31] the shell composed of crosslinked PILs and MA is generated onto the surface of the calcium hydroxide particle by free radical polymerization. After being encapsulated with polymer shell, the surface of the microcapsules became smooth (Fig. 2c). The core–shell structure can be distinguished from the original $Ca(OH)_2$ particles by TEM image (Fig. 2b and d). The EDX (inset of Fig. 2a and c), FTIR (Fig. 3) and XRD (Fig. 4) were used to
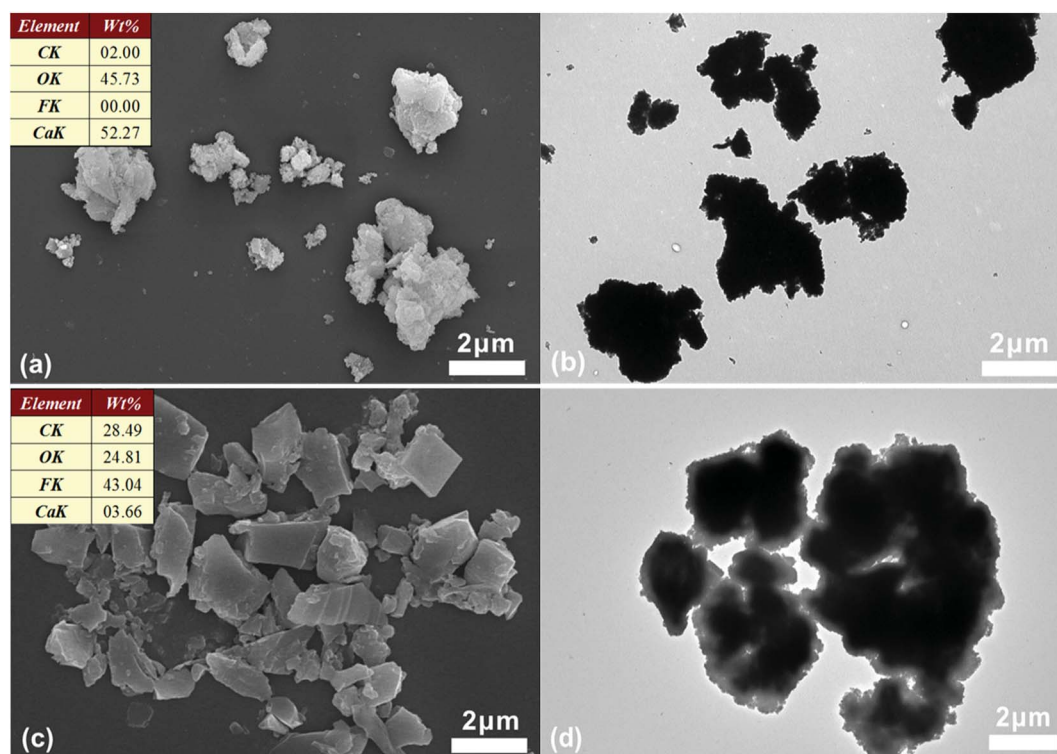

Fig. 2 The morphological observations: the SEM (a) and TEM (b) images of Ca(OH)$_2$. The SEM (c) and TEM (d) images of microcapsules. The inset of (a) and (c) shows the elemental composition obtained from EDX analysis.

confirm the composition and structure of the microcapsules. The $Ca(OH)_2$ shows a broad peak at 3642 cm^{-1}, corresponding to the stretching vibration of O–H. The same peak was also observed in the FTIR spectra of microcapsules. The band at 1642 cm^{-1} can be attributed to the imidazolium cation. The characteristic band at 843 cm^{-1} refers to hexafluorophosphate (PF_6^-) ions of the ILs. The characteristic band at 2929 cm^{-1} represents the methylene groups. The characteristic band at 1575 cm^{-1} can be assigned to aromatic moieties. Compared to $Ca(OH)_2$, the fluorine and carbon element were detected in microcapsules by EDX, which implies that VEImPF$_6^-$ is the component of the shell. The microcapsules and $Ca(OH)_2$ have shown similar diffraction peaks in the XRD spectra, such as at 2θ of 17.98°, 34.02° and 47.04°, which implies that the structure of $Ca(OH)_2$ remained same after encapsulation.

The controlled release of the microcapsule

The Cl$^-$ ions are quite abundant in the marine environment. The PILs are sensitive to chloride by exchanging the PF_6^- with

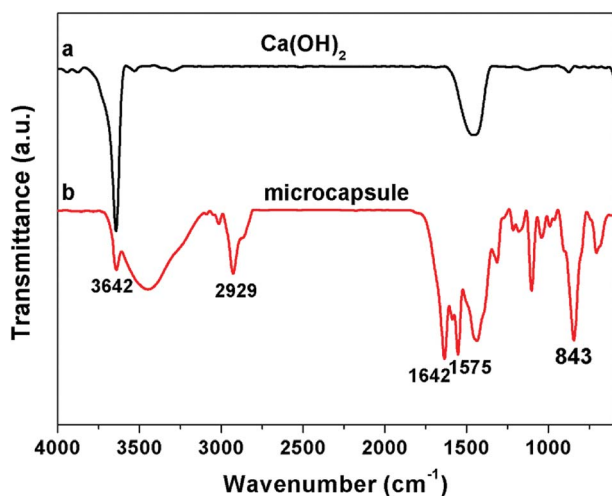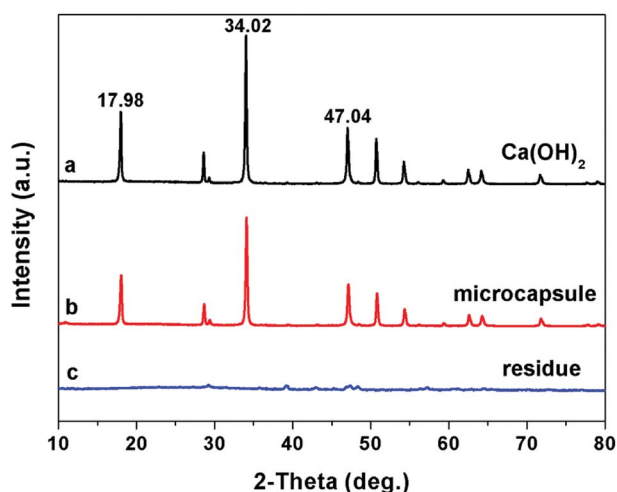Fig. 3 The FTIR spectra of $Ca(OH)_2$ (a) and microcapsule (b).

Fig. 4 The XRD spectra of $Ca(OH)_2$ (a), microcapsule (b) and the residue of microcapsules treated by NaCl solution (c).

Cl$^-$ and can be changed from hydrophobic to hydrophilic, forming hydrophilic channels on the shell. The $Ca(OH)_2$ can penetrate out of the microcapsules through the hydrophilic channels. After soaking in water for 12 h, the morphology of microcapsule remained intact. The surface of the microcapsules was smooth and the composition was same as the original microcapsules (Fig. 5a). The core–shell structure was observed by TEM image, as shown in Fig. 5b. On the other hand, after being immersed in NaCl solution (16.4 mmol L^{-1}) for 10 min, a large number of nanometer-sized holes were observed on the shell of the microcapsules (inset of Fig. 5c). The $Ca(OH)_2$ core partially penetrated out from the microcapsule at this stage (Fig. 5c). After 4 h, only porous polymer shell residue was left (Fig. 5d). The composition of the residue was assessed by EDX (inset of Fig. 5d), which shows a sharp decrease of the fluorine content but a significantly increase of the chlorine content compared with that of the microcapsules. This indicates that the PF_6^- of PILs have been exchanged by Cl$^-$. A little calcium was detected, which implies that $Ca(OH)_2$ has been completely released.

The release process of the microcapsules, triggered by Cl$^-$, has been investigated in detail. The Ca^{2+} ions can combine with MTB in alkaline solution and form a blue complex. The UV-vis spectrometer was used to compare the absorbance of the blue complex with standard calcium solution to calculate the concentration of Ca^{2+}. Fig. 6 presents the concentration of OH$^-$ and Ca^{2+} in 12 mg of microcapsules, immersed in 30 mL of NaCl solution (8.7 mmol L^{-1}). The concentration of OH$^-$ and Ca^{2+} immediately increased when the microcapsules were added to the solution, which indicates that the Cl$^-$ can be rapidly exchanged with the PF_6^- of the PILs. The PILs on the shell of the microcapsules became hydrophilic, forming hydrophilic channels for $Ca(OH)_2$ transport. The concentration of OH$^-$ and Ca^{2+} in the suspension reached a stable level within 1 h. The $Ca(OH)_2$ was completely released in 1 h, reaching 3 mmol L^{-1} of Ca^{2+} in water. The XRD spectra confirmed the absence of $Ca(OH)_2$ from the residue sample after the release process (Fig. 4c). No more calcium was released even with hydrochloric acid (HCl) addition, which indicates that the microcapsules have been depleted.

The microcapsules with different contents of ILs were synthesized. In a typical release process, 12 mg of the microcapsules were added to 30 mL of NaCl aqueous solution. The concentration of Cl$^-$ was 8.7 mmol L^{-1}. As shown in Fig. 7a, for the microcapsules with a shell composed of pure PILs, the release of $Ca(OH)_2$ was close to the dissolution of bare $Ca(OH)_2$ particles. When the microcapsules were immersed in NaCl aqueous solution, the PF_6^- was exchanged with Cl$^-$, causing the hydrophobic PILs to convert into hydrophilic. The linear hydrophilic PILs can be dissolved in water. Thus, the shell of the microcapsules collapsed as soon as the microcapsules were added to the NaCl aqueous solution. Hence, DVB is required as a crosslinking agent to control the release rate of $Ca(OH)_2$. As expected, the experimental results demonstrate that the release rate decreased with the increase of DVB content. When the ILs/DVB ratio was changed from 9 : 1 to 1 : 9, the release rate significantly decreased. When the ILs/DVB ratio was 9 : 1, the
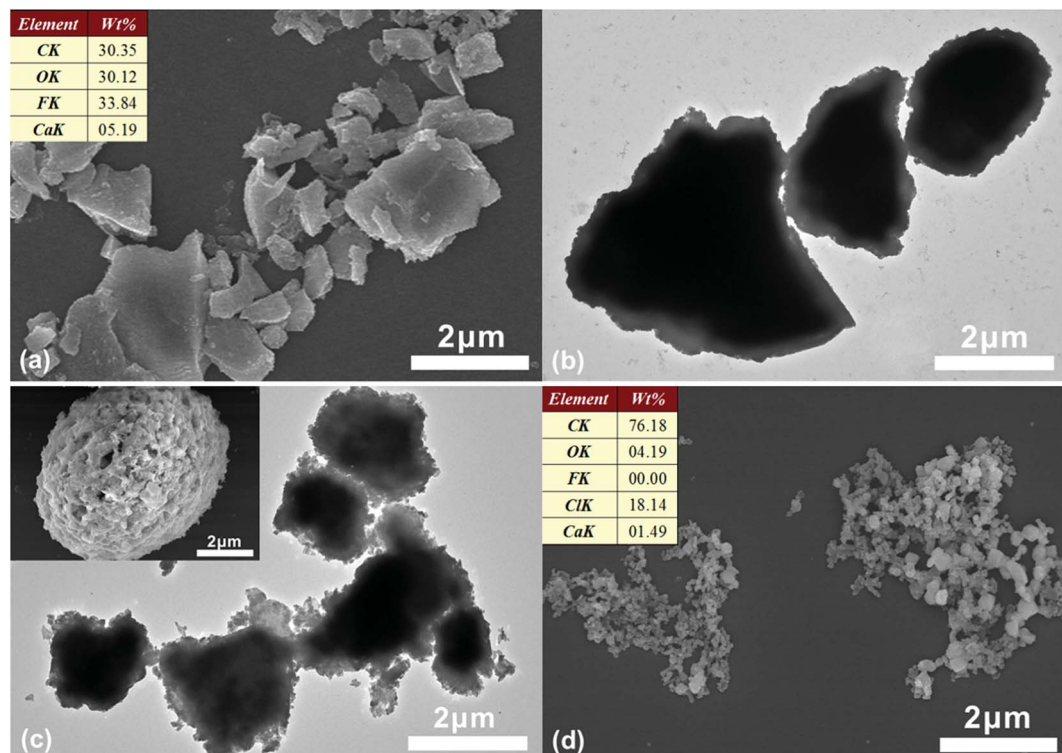
Element	Wt%
CK	30.35
OK	30.12
FK	33.84
CaK	05.19

Element	Wt%
CK	76.18
OK	04.19
FK	00.00
ClK	18.14
CaK	01.49

Fig. 5 The SEM (a) and TEM (b) images of the microcapsules immersed in water. The TEM (c) and SEM (inset of c) images of the microcapsules after being immersed in NaCl solution for 10 min and SEM (d) image of the microcapsules immersed in NaCl solution for 4 h. The inset of (a) and (d) shows the elemental composition obtained from EDX analysis.
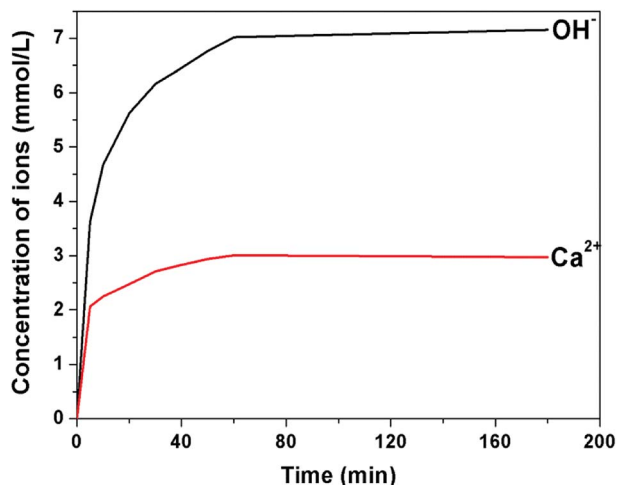

Fig. 6 The concentration of Ca^{2+} and OH^- released by the microcapsules with respect to time. The release process was triggered by NaCl solution.

Ca^{2+} quickly released in first 10 min and reached a maximum level within 0.5 h, which was about 3 mmol L^{-1}. When the ILs/DVB ratio was 1 : 9, the maximum Ca^{2+} concentration was attained in 1.5 h, which was much slower. The DVB is a hydrophobic monomer, whereas the ILs contributes to the hydrophilic zone on the shell of the microcapsules. The higher content of ILs corresponds to a large number of hydrophilic regions, which facilitates the $Ca(OH)_2$ release process. In addition, the channels on the shell of the microcapsules were larger when DVB content is lower (Fig. S1†). The maximum amount of Ca^{2+} released by different microcapsules was almost same. The concentration of Ca^{2+} dissolved by bare $Ca(OH)_2$ powder, with the same weight as microcapsules, was measured. Within 10 min, the concentration of Ca^{2+} reached a maximum of 4.1 mmol L^{-1}. It can be calculated that the $Ca(OH)_2$ accounts for 72.2 wt% of microcapsules.

In addition, we have investigated the influence of the crosslinkage degree on the release rate of Ca^{2+}. The DVB serves as the crosslinking reagent, whereas its monofunctional counterpart, St, was added to tune the degree of crosslinking. The ratio of ILs/hydrophobic monomer (DVB and St) was fixed at 1 : 4 and the ratio of DVB/St was changed from 8 : 0 to 0 : 8. The influence of crosslinking reagent content on Ca^{2+} release process was investigated. The Ca^{2+} release rate decreased when the content of DVB increased (Fig. 7b). When the monomers were comprised of ILs and St, without DVB, the release rate of Ca^{2+} was extremely high, which is similar to the microcapsules composed of pure ILs. The ILs and St are both linear monomers and during the exchange of PF_6^- with Cl^-, the hydrophilic PILs can be transferred into the water. Hence, the shell of the microcapsules immediately disintegrates. Therefore, the encapsulated $Ca(OH)_2$ can dissolve in water as quickly as bare $Ca(OH)_2$ particles. When a low amount of DVB (≤10 wt% of monomers) is added, St segments can be stretched into the water by ILs segments, forming larger holes on the shell (Fig. S2a†). When more DVB is added, the ILs segments obtain
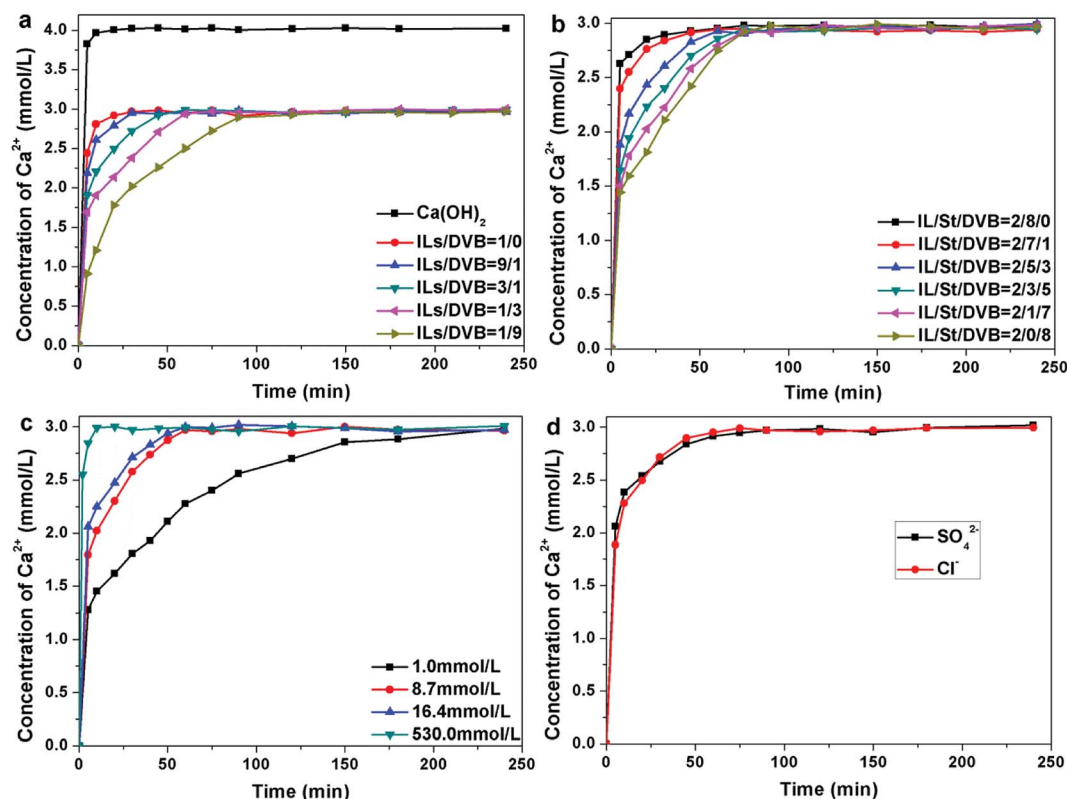
Fig. 7 The concentration of Ca^{2+} released by bare $Ca(OH)_2$ powder and microcapsules with respect to time for different ratios of ILs/DVB (a). The concentration of Ca^{2+} released by microcapsules with respect to time for different ratios of St/DVB (b). The concentration of Ca^{2+} released by microcapsules with respect to time, which is triggered by different amounts of Cl^- (c). The concentration of Ca^{2+} released from microcapsule triggered by SO_4^{2-} (d).

tightly bonded by DVB. The holes on the shell were much smaller (Fig. S2b†), resulting in a slower release rate. As the content of $Ca(OH)_2$ in the microcapsules was the same, the concentration of Ca^{2+} released by different samples was equal.

Furthermore, we aimed to investigate the influence of external factors, such as the concentration of Cl^-. The ratio of ILs/DVB was fixed at 1 : 1. The microcapsules were added in NaCl aqueous solution with different concentrations. We have observed an increase in release rate with the concentration of Cl^- increasing (Fig. 7c). When the concentration of Cl^- was 1 mmol L^{-1}, the Ca^{2+} released slowly and reached the maximum level in 2.5 h. However, when the concentration of Cl^- was increased to 8.7 mmol L^{-1}, the maximum Ca^{2+} concentration was attained within 1 h. When the concentration of Cl^- was increased to 16.4 mmol L^{-1}, the release rate was slightly increased. When the concentration of Cl^- was 530 mmol L^{-1}, which is equivalent to the seawater, the maximum Ca^{2+} concentration was attained in only 10 min. The maximum concentrations of Ca^{2+} triggered by different Cl^- concentrations remained constant.

The responsiveness of microcapsule to SO_4^{2-} was also investigated (Fig. 7d). The SO_4^{2-} can trigger the microcapsules as quickly as Cl^- and the release progress of microcapsule triggered by SO_4^{2-} is similar with that by Cl^-. The anions in the seawater are consists of SO_4^{2-} and Cl^- and both of them can trigger the microcapsules and facilitate the release process. In

our experiment, the release process was triggered by Cl^-. By changing the PF_6^- of PILs with Cl^-, the local concentration of Cl^- was speculated to be decreased. 150 mg of the microcapsules were added to 30 mL NaCl solution (8.7 mmol L^{-1}). The concentration of Cl^- of the suspension was recorded by the Cl^- tester (Fig. 8). The Cl^- concentration decreased from 8.7 mmol L^{-1} to 6 mmol L^{-1} in 40 min. The decrease in Cl^- concentration in the local area around the microcapsules resulted in the decrease of Cl^- content in the suspension. The decrease in Cl^- content in the local area is more obvious, but the measurement process is extremely difficult. At the same time, the content of OH^- in the local area increased due to the release process of microcapsules. Hence, the Cl^-/OH^- ratio around the microcapsules sharply decreased, which can improve the corrosion resistance of the steel in the marine environment.

Furthermore, it can be calculated from the experimental data that the calcium release process follows the modified first-order kinetic model, which is a classical model used to describe the water-soluble substance permeation from porous matrices. The general expression is given below:[32]

$$\ln(100 - F) = -kt + c \qquad (1)$$

where F is the percentage of $Ca(OH)_2$ released at time t. The concentration of Ca^{2+} reached the highest level after a period of time. The Ca^{2+} concentration barely changed with
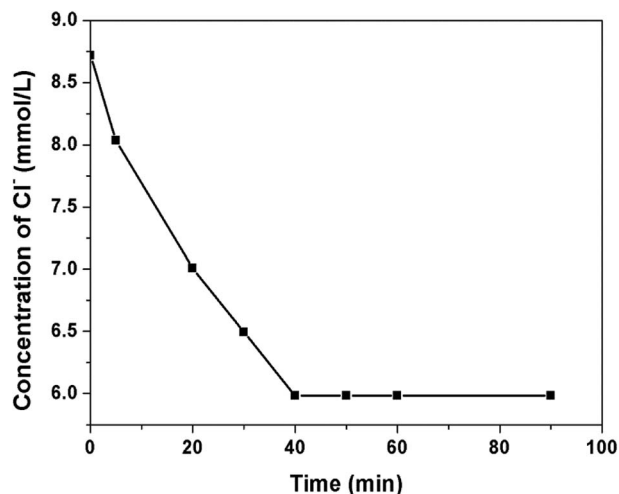
Fig. 8 The concentration of Cl⁻ in NaCl solution after the addition of microcapsules.

hydrochloride acid addition to the dispersion, indicating that the $Ca(OH)_2$ in the microcapsule has been completely released. Therefore, the F value can be calculated by comparing the concentration of Ca^{2+} at time t to the highest concentration. k is the permeability constant. By constructing a natural logarithmic plot of $(100 - F)$ with respect to time, the microcapsule permeability can be calculated from the slope of the resulting linear line. The calculated parameters are presented in Table 1. The correlation coefficient (R^2) was higher than 0.93 for all the samples, except those with no DVB or less DVB, indicating that the release process of $Ca(OH)_2$ from the microcapsules followed the first-order kinetic model. It can be observed that the permeability coefficient k decreased with an increase in DVB content.

Corrosion resistance of Q235 steel

To investigate the corrosion resistance of the microcapsule, the Q235 steel was used in this study. Four steel bars were

immersed in acetone for 5 h and then wrapped with water repellent tape. The top and bottom surfaces remained exposed. The epoxy resin was coated on the tape to repel water. One end of the steel bar was connected to the wire and other end was exposed for corrosion. The steel side without wire, used as the working electrode, was immersed in simulated seawater (3.5 wt% NaCl solution) with different amounts of microcapsules for 60 d at room temperature. The content of the microcapsules for these experiments and the resulting images are shown in Fig. 9. The steel bar without microcapsules was severely corroded in NaCl solution (Fig. 9a). However, the steel bar with 1.5 g of microcapsules remained un-corroded in NaCl solution, which demonstrates the desirable influence of microcapsules on corrosion behaviour (Fig. 9d).

Furthermore, the quantitative assessment of corrosion resistance was carried out by estimating the mass loss of steel bar in 6 wt% NaCl solution with different amounts of microcapsules. Although the relatively high concentration of Cl⁻ was used to investigate the corrosion inhibition capability of microcapsules, the results obtained under accelerated conditions are expected to remain similar with the results under natural corrosion conditions. After 20 d, the steel has been severely corroded in NaCl solution without microcapsules (Fig. S3†). Then, the steel bars were taken out from NaCl solution and weighed. Based on the data obtained by weighing, the mass loss of steel can be calculated as follows:[33]

$$\Delta m_{\mathrm{grav}} = m_{\mathrm{o,grav}} - m_{\mathrm{i,grav}} \tag{2}$$

where Δm_{grav} is the gravimetric mass loss, $m_{\mathrm{o,grav}}$ and $m_{\mathrm{i,grav}}$ are the mass of steel before and after corrosion, respectively. Table
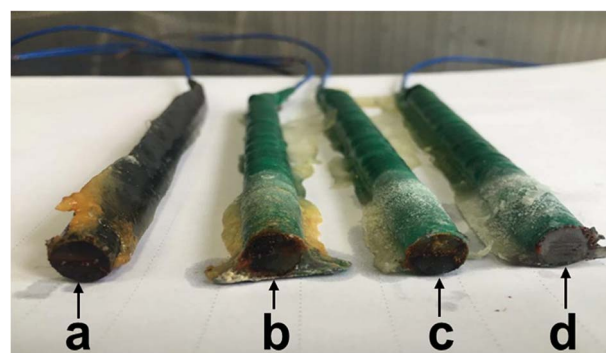

Fig. 9 The digital photograph of the steel samples with different contents of microcapsules in simulated seawater after 60 d: 0 g (a), 0.5 g (b), 1 g (c), 1.5 g (d).

Table 1 The kinetic parameters, calculated from the first-order model, for the release of $Ca(OH)_2$ from microcapsules

ILs/DVB	1 : 0	9 : 1	3 : 1	1 : 1	1 : 3	1 : 9
R^2	0.8982	0.9447	0.9557	0.9678	0.9573	0.9704
k	0.1377	0.1231	0.0709	0.0654	0.0584	0.0326

ILs/St/DVB	2 : 8 : 0	2 : 7 : 1	2 : 5 : 3	2 : 3 : 5	2 : 1 : 7	2 : 0 : 8
R^2	0.7476	0.8505	0.9574	0.9573	0.9656	0.9453
k	0.0569	0.0573	0.0544	0.0468	0.0427	0.0412

cCl⁻ (mmol L⁻¹)		16.4	8.7	4.0	2.0	1.0
R^2		0.9369	0.9503	0.9637	0.9881	0.9806
k		0.0653	0.0533	0.0297	0.0236	0.0168

Table 2 The results obtained from the gravimetric method

Content of microcapsule (g)	$m_{\mathrm{o,grav}}$ (g)	$m_{\mathrm{i,grav}}$ (g)	Δm_{grav} (g)
0	2.4873	2.4509	0.0364
0.5	2.4858	2.4652	0.0206
1	2.5099	2.4974	0.0125
1.5	2.5206	2.5104	0.0102

2 shows the mass loss of steel. One should note that the Δm_{grav} of steel immersed in simulated seawater without microcapsules was larger than the steel in the presence of microcapsules, which implies that microcapsules enhanced corrosion resistance of steel. Moreover, the mass loss of steel bar has shown an inverse relationship with the content of microcapsules, which suggests that higher content of microcapsules effectively inhibit the corrosion of steel.

Conclusions

We have demonstrated a facile process to achieve large-scale synthesis of anion sensitive $Ca(OH)_2$ microcapsules, which can be used to enhance the corrosion resistance of steel under marine environment. By exchanging the PF_6^- with Cl^- in water, the hydrophobic PILs on the shell can be changed to hydrophilic channels on the shell of the microcapsules. The release of $Ca(OH)_2$ caused an increase of OH^- concentration. The concentration of Cl^- was lowered by exchanging with PF_6^-. Hence, the Cl^-/OH^- ratio can be reduced, which improves the corrosion resistance of steel. The release rate of $Ca(OH)_2$ has shown a direct relationship with ILs content and an inverse relationship with DVB content. Meanwhile, the decrease of Cl^- concentration in the water can result in the decreased release rate of $Ca(OH)_2$. However, the maximum amount of Ca^{2+} released by different microcapsules or triggered by different Cl^- concentration was almost same. The release rate of $Ca(OH)_2$ from the microcapsules followed the first-order kinetic model. In addition, SO_4^{2-} can also trigger the release of $Ca(OH)_2$. The enhanced corrosion resistance in simulated marine water has been demonstrated. After the addition of microcapsules, the steel remained un-corroded for 60 d. The mass loss of steel immersed in NaCl solution significantly decreased due to the presence of microcapsules. The novel microcapsules are promising due to large-scale synthesis and improved corrosion resistance of steel bars, which can improve the durability of reinforced concrete structures. In addition, the proposed synthesis process can be extended to encapsulate other corrosion inhibitors and functional materials for a wide range of applications.

Conflicts of interest

There are no conflicts of interest to declare.

Acknowledgements

Notes and references

1 C. L. Page, *Nature*, 1975, **258**, 514–515.

2 C. L. Page and K. W. J. Treadaway, *Nature*, 1982, **297**, 109–115.

3 S. Ahmad, *Cem. Concr. Compos.*, 2003, **25**, 459–471.

4 M. Sahmaran, *J. Mater. Sci.*, 2007, **42**, 9131–9136.

5 W. M. Zhang and H. J. Ba, *J. Mater. Civ. Eng.*, 2011, **23**, 330–334.

6 N. Etteyeb, L. Dhouibi, M. Sanchez, C. Alonso, C. Andrade and E. Triki, *J. Mater. Sci.*, 2007, **42**, 4721–4730.

7 G. Falzone, M. Balonis, D. Bentz, S. Jones and G. Sant, *Cem. Concr. Res.*, 2017, **101**, 82–92.

8 J. Liu, Q. W. Qiu, X. C. Chen, X. D. Wang, F. Xing, N. X. Han and Y. J. He, *Corros. Sci.*, 2016, **112**, 364–372.

9 J. X. Xu, L. H. Jiang and J. X. Wang, *Constr. Build. Mater.*, 2009, **23**, 1902–1908.

10 Y. H. Cao, S. G. Dong, D. J. Zheng, J. J. Wang, X. J. Zhang, R. G. Du, G. L. Song and C. J. Lin, *Corros. Sci.*, 2017, **126**, 166–179.

11 S. Muthulingam and B. N. Rao, *Corros. Sci.*, 2014, **82**, 304–315.

12 K. Thangavel and N. S. Rengaswamy, *Cem. Concr. Compos.*, 1998, **20**, 283–292.

13 U. Angst, B. Elsener, C. K. Larsen and Ø. Vennesland, *Cem. Concr. Res.*, 2009, **39**, 1122–1138.

14 H. Yu, K. T. K. Chiang and L. Yang, *Constr. Build. Mater.*, 2012, **26**, 723–729.

15 H. L. Huang and G. Ye, *J. Intell. Mater. Syst. Struct.*, 2015, **26**, 309–320.

16 A. La Iglesia, V. M. La Iglesia, S. Fajardo, P. P. Gómez and J. M. Bastidas, *Constr. Build. Mater.*, 2012, **37**, 46–50.

17 Y. S. Wang, W. J. Ding, G. H. Fang, Y. Q. Liu, F. Xing and B. Q. Dong, *Constr. Build. Mater.*, 2016, **125**, 742–748.

18 T. Matsuda, N. Jadhav, K. B. Kashi, M. Jensen, A. Suryawanshi and V. J. Gelling, *Prog. Org. Coat.*, 2016, **90**, 425–430.

19 Y. He, W. Xu, R. Tang, C. L. Zhang and Q. B. Yang, *RSC Adv.*, 2015, **5**, 90609–90620.

20 Y. S. Wang, G. H. Fang, W. J. Ding, N. X. Han, F. Xing and B. Q. Dong, *Sci. Rep.*, 2015, **5**, 18484–18491.

21 J. Y. Wang, H. Soens, W. Verstraete and N. D. Belie, *Cem. Concr. Res.*, 2014, **56**, 139–152.

22 Z. X. Yang, J. Hollar, X. D. He and X. M. Shi, *Cem. Concr. Compos.*, 2011, **33**, 506–512.

23 J. Bujes-Garrido and M. J. Arcos-Martinez, *Talanta*, 2016, **155**, 153–157.

24 W. Xiong, J. N. Tang, G. M. Zhu, N. X. Han, E. Schlangen, B. Q. Dong, X. F. Wang and F. Xing, *Sci. Rep.*, 2015, **5**, 10866–10871.

25 X. Y. Ji, Q. Zhang, F. X. Liang, Q. N. Chen, X. Z. Qu, C. L. Zhang, Q. Wang, J. L. Li, X. M. Song and Z. Z. Yang, *Chem. Commun.*, 2014, **50**, 5706–5709.

26 T. Ueki and M. Watanabe, *Macromolecules*, 2008, **41**, 3739–3749.

27 J. Qin, X. Q. Zou, S. T. Lv, Q. Z. Jin and X. G. Wang, *RSC Adv.*, 2016, **6**, 87703–87709.

28 X. Y. He, W. Yang and X. W. Pei, *Macromolecules*, 2008, **41**, 4615–4621.

29 D. G. Themelis, P. D. Tzanavaras, A. N. Anthemidis and J. A. Stratis, *Anal. Chim. Acta*, 1999, **402**, 259–266.

30 T. Zafeiropoulou, E. Rakanta and G. Batis, *Prog. Org. Coat.*, 2011, **72**, 175–180.

31 P. Zhou, Q. Wang, C. L. Zhang, F. X. Liang, X. Z. Qu, J. L. Li and Z. Z. Yang, *Chin. Chem. Lett.*, 2015, **26**, 657–661.

32 S. Dash, P. N. Murthy, L. Nath and P. Chowdhury, *Acta Pol. Pharm.*, 2010, **67**, 217–223.

33 M. Beck, J. Goebbels, A. Burkert, B. Isecke and R. Bäßler, *Mater. Corros.*, 2010, **61**, 475–479.